Cooperative Control for Localization of Mobile Sensor Networks

Fan Zhang, Ben Grocholsky, Vijay Kumar, and Max Mintz

GRASP Laboratory, University of Pennsylvania, Philadelphia, PA 19104, USA
{zhangfan,bpg,kumar,mintz}@grasp.cis.upenn.edu

Summary. In this paper, we consider the problem of cooperatively control a formation of networked mobile robots/vehicles to optimize the relative and absolute localization performance in 1D and 2D space. A framework for active perception is presented utilizing a graphical representation of sensory information obtained from the robot network. Performance measures are proposed that capture the estimate quality of team localization. We show that these measures directly depend on the sensing graph and *shape* of the formation. This dependence motivates implementation of a gradient based control scheme to adapt the formation geometry in order to optimize team localization performance. This approach is illustrated through application to a cooperative target localization problem involving a small robot team. Simulation results are presented using experimentally validated noise models.

1 Introduction

In order for a team of mobile robots to navigate autonomously and perform such cooperative tasks as manipulation, surveillance, or search and rescue, they must be able to localize themselves relative to each other as well as relative to a global reference frame. Therefore, how to estimate robots' and/or targets' positions in a precise and efficient way is a crucial factor that impacts the overall performance of mobile robot platforms. In this paper, we are interested in situations where sensors are placed on networked mobile robots that can be thought of as a sensor network with additional degrees of freedom afforded by mobility. We assume that robots within a team can communicate and combine mutual sensor measurements, such as relative range and bearing, to improve their localization performance, and further investigate how to control robots' motions cooperatively in order to optimize the performance of such localization process.

The approach presented in this paper is closely related to and builds on three threads of recent research. The first is localization of a team of robots [1, 2, 3] where distributed robot measurements from heterogeneous sensors are

integrated and fused to localize all the robots in the team. Second, in addition to localizing robots, it may also be essential to localize targets. Different approaches to track targets are described in [4, 5, 6]. For example, robots are driven by controllers designed to minimize the errors associated with estimates of target locations. Thus, optimal trajectories for mobile robots to localize or track the targets can be obtained assuming that the robots' states are known exactly [5, 6]. Third, more generally, a team of robots can be controlled to perform a wide range of tasks including, for example, manipulation [7] and surveillance [8]. The cooperative control of multi-robot formations is addressed in [9, 10, 11, 12].

In most of these papers, controllers to regulate the shape of the formation are described. The control of shape to maintain constraints due to communication and sensing is addressed by [13]. Similarly, constraints on the shape to accomplish cooperative manipulation tasks are described in [7].

In all three problem areas, it is necessary to model the interaction (sensing, communication, and physical constraints) between robots. Graphs are the natural mathematical objects for modeling these discrete interactions [11, 14]. Results on graph rigidity theory [15, 16, 17] can be directly applied to localization of multi-robot systems in $\mathbb{R}^2$ and $\mathbb{SE}(2)$ in a deterministic setting [18, 19]. In particular, directed graphs in which edges model the observations of one robot by another robot can be used to model a robot network [20].

Our focus in this paper is on the dependence of localization errors on the robots' states or the shape of the formation and the information available to each robot. We consider the scenario in which the positions of robots and targets are estimated simultaneously from distributed sensor measurements. We address the problem of localizing robots in addition to targets, and controlling the robots by optimizing an appropriate measure of performance. Our performance metric for localization is based on the uncertainty associated with the estimates of relative or absolute positions of the robots and targets.

This paper is organized as follows. In Section 2, we present a model for formations of mobile sensor networks, incorporating observations of robots and targets by other robots and the errors associated with these observations. In Section 3, we discuss models for sensors with a particular emphasis on cameras. We derive a simple state-dependent measurement noise model for omni-directional cameras. The connection between measurement errors and estimate uncertainty is introduced in Section 4, and the dependence of localization quality on formation geometry is also investigated. We derive a simple controller that drives the team of robots to locally optimal formations in Section 5, with applications of these concepts to a small team of robots in $\mathbb{R}$ and $\mathbb{R}^2$. We discuss some of the advantages of the proposed approach and the key challenges for future research in Section 6.

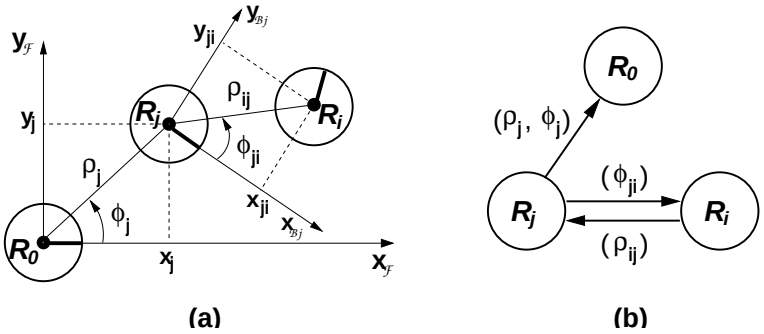

Fig. 1. Modeling of sensory information (an example in $\mathbb{R}^2$): (a) A team of two robots in $\mathbb{R}^2$: R_i has range measurements about R_j; R_j has absolute measurements about itself and bearing measurements about R_i. A body reference frame, $\mathcal{B}_j$, has been attached to R_j. (b) The sensing graph representation of the team in (a).

2 Modeling of Sensor Networks

Consider a d-dimensional Euclidean world, $\mathcal{W} = \mathbb{R}^d$ ($d = 1$ or 2), occupied by a team of n robots, $\mathcal{R} = \{R_1, R_2, \ldots R_n\}$, and assume each robot can communicate with every other robot in the team. The physical configurations of the robots coupled with the characteristics of the hardware and the requirements of the sensing and control algorithms induce a *physical network* or a *formation* of n robots in $\mathbb{R}^d$. We define a global reference frame $\mathcal{F}$ by defining a virtual robot or a beacon R_0 with fixed position $\mathbf{x}_0 = 0$ in the inertial frame. (See Figure 1(a)). The *shape* of the formation in $\mathcal{F}$ is denoted by shape variable $\mathbf{x} = \left[\mathbf{x}_1^T, \mathbf{x}_2^T, \ldots, \mathbf{x}_n^T\right]^T \in \mathbb{R}^{dn}$, where $\mathbf{x}_i \in \mathbb{R}^d$ is the position vector of the i^{th} robot in $\mathcal{F}$. A body reference frame $\mathcal{B}_j$ at the j^{th} robot is also defined with its x-axis aligned with the direction of heading of R_j. The shape of the formation in the body-fixed frame $\mathcal{B}_j$ is described by $\tilde{\mathbf{x}} = [(\mathbf{x}_1^j)^T, (\mathbf{x}_2^j)^T, \ldots, (\mathbf{x}_n^j)^T]^T$, where $\mathbf{x}_i^j$ is the relative position vector of R_i about R_j, and $\mathbf{x}_j^j = 0$. For a formation of n robots in $\mathbb{R}^d$, localization is the determination of the $d \cdot n$ coordinates in $\mathbf{x}$ or $\tilde{\mathbf{x}}$ that characterize the robots' positions in a particular reference frame.

2.1 Sensing Graph

In order to represent the sensory information, we define a directed graph called the *sensing graph*, $\mathcal{G} = (\mathcal{V}, \mathcal{E}, \mathcal{Z}, \mathcal{P})$, where $\mathcal{V} = \mathcal{R} \cup \{R_0\}$ is a finite set of vertices. The edge set $\mathcal{E} \subset \mathcal{V} \times \mathcal{V}$ consists of labeled, directed edges that represent the presence of measurements (observations) between robots. An arrow emanating from R_i leading to R_j indicates one or more sensor measurements of R_j made by R_i. In this paper, we consider three types of exteroceptive sensors: range sensors, bearing sensors, and global positioning sensors. Thus,

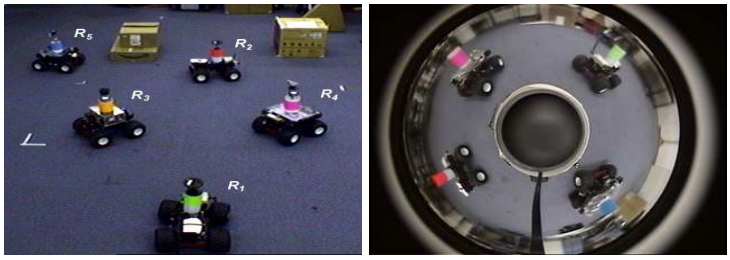

Fig. 2. A formation of five car-like mobile robots (left) and a sample image from omni-directional camera sensor (right).

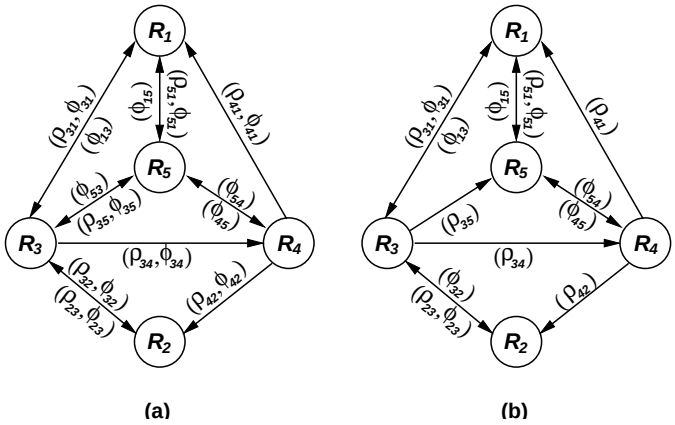

Fig. 3. Two candidate sensing graphs for the five-robot formation. In (a), the measurement set $\mathcal{Z}$ =$\{$ ϕ_{13}, ϕ_{15}, ρ_{23}, ϕ_{23}, ρ_{31}, ρ_{32}, ρ_{34}, ρ_{35}, ϕ_{31}, ϕ_{32}, ϕ_{34}, ϕ_{35}, ρ_{41}, ρ_{42}, ϕ_{41}, ϕ_{42}, ϕ_{45}, ρ_{51}, ϕ_{51}, ϕ_{53}, ϕ_{54} $\}$, while in (b) the measurement set $\mathcal{Z}$ =$\{$ ϕ_{13}, ϕ_{15}, ρ_{23}, ϕ_{23}, ρ_{31}, ρ_{34}, ρ_{35}, ϕ_{31}, ϕ_{32}, ρ_{41}, ρ_{42}, ϕ_{45}, ρ_{51}, ϕ_{51}, ϕ_{54} $\}$.

the measurement set $\mathcal{Z}$ consists of three types of sensory information: (i) the range between two robots, ρ_{ij}, (ii) the bearing of one robot in relation to another, ϕ_{ij}, and (iii) the absolute position of a robot in $\mathcal{F}$, $\mathbf{x}_j$, which can be obtained either by global positioning sensors, or by triangulation with some fixed, known landmarks. The set $\mathcal{P}$ contains the uncertainties associated with the measurements in $\mathcal{Z}$.

An example of a team of two robots, R_i and R_j, with a fixed beacon R_0, is shown in Figure 1(a). The directed, labeled sensing graph for the team is shown in Figure 1(b). More generally, in a sensing graph $\mathcal{G}$, the j^{th} vertex has an incoming edge from the i^{th} vertex whenever robot R_i can sense robot R_j. Corresponding to different types of sensory information, we use the following labels: (i) (ρ_{ij}) or $(\rho_{ij}, null)$ to denote a range measurement, (ii) (ϕ_{ij}) or $(null, \phi_{ij})$ to denote a bearing measurement, and (iii) (ρ_{ij}, ϕ_{ij}) to denote a

range-bearing measurement. Any absolute measurement made by any robot R_j can be represented by a directed edge from R_j to R_0.

A second example of a formation of a five-robot team is shown in Figure 2. Figure 3 gives two candidate sensing graphs for this formation that are constructed by two different sets of relative measurements.

2.2 Observation Models

Each range and bearing measurement in $\mathcal{Z}$, which can be potentially used to estimate the relative distance or angles between the robots, provides information about the shape of a multi-robot formation. Thus, every range and bearing measurement in the associated sensing graph $\mathcal{G}$ can be written as an observation equation on the shape variable, $\mathbf{x}$ or $\tilde{\mathbf{x}}$, of the formation.

Specifically, for a formation of robots in $\mathbb{R}$, all measurements in $\mathcal{Z}$ lead to an observation model on the relative positions of the form:

$$\rho_{ij} = |x_i - x_j| \,, \tag{1}$$

where x_i and x_j are the positions of robot R_i and R_j in $\mathbb{R}$ respectively.

For a multi-robot formation in $\mathbb{R}^2$, measurements lead to one of three types of observation models on the shape variables. For a pair of robots, in a body-fixed reference frame $\mathcal{B}_j$:

$$\text{Type 1}: \;\; \rho_{ik} = \sqrt{(\mathbf{x}_i^j - \mathbf{x}_k^j)^T(\mathbf{x}_i^j - \mathbf{x}_k^j)} \,, \tag{2}$$

$$\text{Type 2}: \;\; \phi_{ji} = tan^{-1}(y_i^j / x_i^j) \,. \tag{3}$$

For a group of three robots R_i, R_j, and R_k, a pair of bearing measurements, ϕ_{ij} and ϕ_{ik}, results in the following Type 3 observation model.

$$\text{Type 3}: \;\; \phi_{ij} - \phi_{ik} = cos^{-1} \frac{(\mathbf{x}_i^j - \mathbf{x}_j^j)^T(\mathbf{x}_i^j - \mathbf{x}_k^j)}{\|\mathbf{x}_i^j - \mathbf{x}_j^j\| \cdot \|\mathbf{x}_i^j - \mathbf{x}_k^j\|} \,. \tag{4}$$

And all these observation models, Equations (1–4), can be written in the form

$$\mathbf{z} = \mathbf{h}(\tilde{\mathbf{x}}) \,, \tag{5}$$

where $\mathbf{z} = \mathbf{A}\,\mathbf{z}_0$ with $\mathbf{z}_0$ be a vector of p measurements in the set $\mathcal{Z}$ and $\mathbf{A}$ is a $m \times p$ matrix whose elements are either 1, -1 or 0, and $\mathbf{h}$ is a nonlinear function of the shape variable in a body-fixed reference frame. Choosing R_0 as the origin, the above observation equations can be also written in terms of absolute coordinates $\mathbf{x}$ with respect to a global reference frame.

These are the only three types of observation models that can be used to describe the network in $\mathbb{R}$ or $\mathbb{R}^2$. All other equations that can be written are functionally dependent on the above observation equations.

Given a formation of n robots in $\mathbb{R}^d$, it is necessary to first check if $d \cdot n$ independent observation equations are available to determine the $d \cdot n$ coordinates in the shape variable $\mathbf{x}$ or $\tilde{\mathbf{x}}$. In [20], we have developed a test of functional independence for all observations by defining a constraint matrix that is built by the derivatives of those observation equations.

3 Sensor Models

3.1 Introduction

While Equations (1–4) describe the geometry of the team robots, they do not incorporate the measurement noise that is inherent in the process. We modify Equation (5) to incorporate the measurement noise, $\mathbf{v}$:

$$\mathbf{z} = \mathbf{h}(\tilde{\mathbf{x}}, \mathbf{v}) \ , \tag{6}$$

The above equation is general enough to model typical sensors on mobile robots, including global position systems (GPS), inertial measurement units (IMUs), ultrasonic or infra-red range sensors, and cameras[1].

In many sensors, the quality of the measurements is often a function of the state of the system. For example, ultrasonic sensors have a sweet spot while camera resolution decreases with range. This suggests that to improve the localization of a team of robots, it is beneficial for robots to move into "optimal" configurations. While it may be difficult to determine what an optimal configuration is, it is certainly meaningful to investigate schemes that might improve the quality of estimates of relative positions by moving the robots relative to each other. Hence we are interested in a control scheme that can improve the estimation quality of robots' and targets' positions by cooperatively moving the robots towards states that are optimal for relative measurements.

In this section we consider indoor mobile robots and cameras as sensors for localization. We investigate omni-directional cameras and use experimental data to develop a sensor model. This will be used as a basis for investigating optimal formations for localization.

3.2 Omni-directional cameras

The omni-directional camera detailed in Figure 4 utilizes a parabolic mirror in order to enable a single camera to directly measure both range and bearing to a feature. The mirror geometry introduces a nonlinear observation model that relates the pixel measurements $z = r_c$ to the range observation $y = r$, given by

[1] In some cases, *e.g.* IMUs, it may be necessary to condition and filter the raw sensory information before it can be written in the above form.

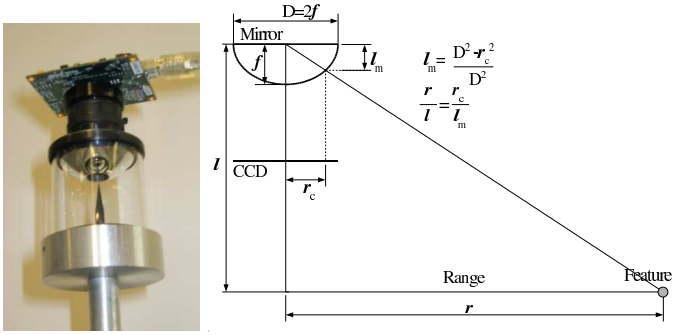

Fig. 4. Parabolic omni-directional camera and geometry

$$z = h(y) + \nu = \frac{D}{y}\left(\sqrt{l^2 + y^2} - l\right) + \nu. \tag{7}$$

where $\nu \sim N(0, R)$ is measurement noise in pixel coordinates. For a given operating condition, the sensitivity of the range observations to small changes in pixel coordinates can be obtained by linearizing Equation (7):

$$H = \frac{\partial h}{\partial y} = \frac{y^2\sqrt{l^2 + y^2}}{Dl\left(\sqrt{l^2 + y^2} - l\right)}. \tag{8}$$

Our experiments show that the noise in pixel measurements is reasonably well modeled by a normal distribution, $N(0, R)$. From Equation (8), this leads to errors in the observations of y given by $(H^T R^{-1} H)^{-1}$. Since H is a function of range, the variance associated with a range observation, $y = \rho_{ij} = \|\mathbf{x}_i - \mathbf{x}_j\|$, obtained from an omni-directional camera, will depend on the range.

The experimental data in Figure 5(a) shows observations for different ranges. In the experiments, an omni-directional camera was rotated about

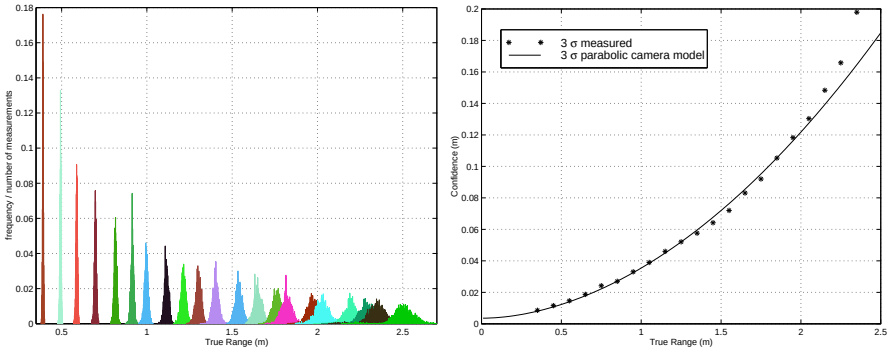

Fig. 5. (a) Omni-directional camera measurements and feature range histogram. (b) Measured and modeled range measurement uncertainty

its vertical axis while observing static features at various known ranges. As the range decreases, the distribution is sharper and the variance associated with the distribution decreases. It is not too hard to see from Equation (8) that the variance is approximately proportional to the fourth power of the range:

$$\sigma^2_{\rho_{ij}} = \sigma_0^2 + \sigma_1^2 \|\mathbf{x}_i - \mathbf{x}_j\|^4 . \tag{9}$$

As shown in Figure 5(b), the predicted range-dependent measurement uncertainty given by Equation (9) (shown by the solid curve) agrees well with the experimental data points.

In the next section, we will define a measure of the quality of localization, and use the model in Equation (9) to develop the dependence of this measure on the geometry of the formation.

4 Measures of Localization

Given the noise model of the camera sensors, we are interested in the connection between measurement errors and estimation errors. We assume that each sensor measurement is taken independently. Accordingly, if the observation models in Equation (5) are linearized about the nominal state, $\mathbf{x_n}$, they can be written in the form:

$$\Delta\mathbf{z} = \left.\frac{\partial \mathbf{h}(\mathbf{x}, \mathbf{v})}{\partial \mathbf{x}}\right|_{\mathbf{x_n}} \Delta\mathbf{x} + \left.\frac{\partial \mathbf{h}(\mathbf{x}, \mathbf{v})}{\partial \mathbf{v}}\right|_{\mathbf{x_n}} \Delta\mathbf{v} \ . \tag{10}$$

We use weighted least squares (WLS) method to obtain the estimates of $\Delta\mathbf{x}$ around the nominal states, $\mathbf{x_n}$, of robots and targets. Defining

$$\mathbf{H}(\mathbf{x}) = \frac{\partial \mathbf{h}(\mathbf{x}, \mathbf{v})}{\partial \mathbf{x}} \quad \text{and} \quad \mathbf{L}(\mathbf{x}) = \frac{\partial \mathbf{h}(\mathbf{x}, \mathbf{v})}{\partial \mathbf{v}} \tag{11}$$

as the Jacobians of the observation equations around the formation shape that is specified by the measurements, $\mathbf{z}$, Equation (10) can be written as

$$\Delta\mathbf{z} = \mathbf{H}(\mathbf{x})\, \Delta\mathbf{x} + \mathbf{v}', \tag{12}$$

where $\mathbf{v}' = \mathbf{L}(\mathbf{x})\, \Delta\mathbf{v}$ is a vector of random variables, $\mathbf{v}' \sim N(\mathbf{0}, \mathbf{R}(\mathbf{x}))$, with its state-dependent covariance matrix $\mathbf{R}(\mathbf{x})$ defined by the expectation of $\mathbf{L}(\mathbf{x})\Delta\mathbf{v}\Delta\mathbf{v}^T\mathbf{L}(\mathbf{x})^T$.

To obtain the covariance matrix for estimation errors, we can also use a simple weighted least squares method to get

$$\Delta\mathbf{x} = (\, \mathbf{H}^T\mathbf{W}\,\mathbf{H}\,)^{-1}\, \mathbf{H}^T\, \mathbf{W}\Delta\mathbf{z} \ , \tag{13}$$

where $\mathbf{W} = \mathbf{R}(\mathbf{x})^{-1}$ is the weight matrix. Squaring both sides of Equation (13) by multiplying both sides of the equation by their respective transposes:

$$\Delta\mathbf{x}\Delta\mathbf{x}^T = (\mathbf{H}^T\,\mathbf{W}\,\mathbf{H})^{-1}\mathbf{H}^T\mathbf{W}\,\Delta\mathbf{z}\,\Delta\mathbf{z}^T\mathbf{W}^T\,\mathbf{H}\,((\mathbf{H}^T\mathbf{W}\,\mathbf{H})^{-1})^T\ . \tag{14}$$

Taking the expectation of the result, we get the covariance matrix as:

$$\mathbf{P} = (\mathbf{H}^T\,\mathbf{W}\,\mathbf{H})^{-1}\,\mathbf{H}^T\,\mathbf{W}\,\mathbf{R}\,\mathbf{W}^T\,\mathbf{H}\,((\mathbf{H}^T\,\mathbf{W}\,\mathbf{H})^{-1})^T\ . \tag{15}$$

Defining the weight matrix $\mathbf{W} = \mathbf{R}(\mathbf{x})^{-1}$, Equation (15) can be simplified to

$$\mathbf{P}(\mathbf{x}) = [\,\mathbf{H}(\mathbf{x})^T\,\mathbf{R}(\mathbf{x})^{-1}\,\mathbf{H}(\mathbf{x})\,]^{-1}\ . \tag{16}$$

In our simple linearized model with independent, Gaussian noise, the covariance matrix $\mathbf{P}$ contains all the information about the errors in localization.

We can now consider any of a number of cost functions derived from this matrix as a metric and controllers that minimize these cost functions. Two such cost functions are the trace and the determinant of $\mathbf{P}$. They are both scalar utility measures that capture the quality of the estimate obtained from a given set of measurements. Since the elements of matrix $\mathbf{H}$ are written in terms of the shape variables, the covariance matrix $\mathbf{P}$ resulting from Equation (16) is naturally dependent on the shape of the formation. Accordingly, we define two cost functions:

$$\mathcal{J}_{\mathbf{I}}\,(\mathbf{x}\,,\,\mathcal{G}) = \mathrm{trace}\,(\mathbf{P}(\mathbf{x})), \quad \text{or} \quad \mathcal{J}_{\mathbf{II}}\,(\mathbf{x}\,,\,\mathcal{G}) = \det\,(\mathbf{P}(\mathbf{x})). \tag{17}$$

We can also see that these errors are bounded for any set of measurements if $\mathbf{H}$ is a nonsingular, square matrix. If a minimal set of observations are available, the $\mathbf{H}$ matrix derived from a set of m independent observation equations ($m = n-1$ or $2n-2$ or $3n-3$ for systems in $\mathbb{R}$, $\mathbb{R}^2$ or $\mathbb{SE}(2)$ respectively) is nonsingular and square. And the matrix norm of $\mathbf{P}$ can be computed as

$$\|\mathbf{P}\| = \|\mathbf{H}^{-1}\,\mathbf{R}\,\mathbf{H}^{-T}\| \leq \|\mathbf{H}^{-1}\|\cdot\|\mathbf{R}\|\cdot\|\mathbf{H}^{-T}\| = \|\mathbf{R}\|\cdot\|\mathbf{H}^{-1}\|^2\ . \tag{18}$$

This implies that for a given sensing graph, the uncertainty of coordinates estimation will explicitly depend on and also be bounded by the measurement quality and the formation shape. If additional redundant measurements are added, $\mathbf{H}$ is no longer square but continues to be full-rank. In such a situation, even though Equation (18) is no longer valid, the same conclusion can be reached.

5 Optimal Formation Deployment

For a given sensing graph, $\mathcal{G}$, gradient descent of the utility measure, $\mathcal{J}$, provides a mechanism to drive the robot network to an optimal spatial shape for relative measurements. Controlling robot velocity according to

$$\dot{\mathbf{x}} = -k\,\nabla_{\mathbf{x}}\mathcal{J}_{\mathbf{I}}\,(\mathbf{x}\,,\,\mathcal{G}) = -k\,\tfrac{\partial}{\partial\mathbf{x}}\,\mathrm{trace}\,(\mathbf{P}(\mathbf{x})) \tag{19}$$

where k is a constant scalar factor, yields trajectories that realize the desired shape of the formation. Using the matrix calculus relations

$$\frac{\partial}{\partial \mathbf{x}} \operatorname{trace}(\mathbf{X}) = \operatorname{trace}\left(\frac{\partial}{\partial \mathbf{x}} \mathbf{X}\right) \text{ and } \frac{\partial}{\partial \mathbf{x}} \mathbf{X} = -\mathbf{X} \frac{\partial}{\partial \mathbf{x}} \left(\mathbf{X}^{-1}\right) \mathbf{X},$$

the control strategy shown as Equation (19) can be written as

$$\begin{aligned} \dot{\mathbf{x}} &= -k \operatorname{trace}\left[-\mathbf{P}\left(\frac{\partial}{\partial \mathbf{x}}\mathbf{H}^T \mathbf{R}^{-1} \mathbf{H} + \mathbf{H}^T \frac{\partial}{\partial \mathbf{x}}\mathbf{R}^{-1} \mathbf{H} + \mathbf{H}^T \mathbf{R}^{-1} \frac{\partial}{\partial \mathbf{x}}\mathbf{H}\right) \mathbf{P}\right] \\ &= k \operatorname{trace}\left[2\,\mathbf{P}\left(\frac{\partial}{\partial \mathbf{x}}\mathbf{H}^T \mathbf{R}^{-1} \mathbf{H}\right) \mathbf{P} + \mathbf{P}\left(\mathbf{H}^T \frac{\partial}{\partial \mathbf{x}}\mathbf{R}^{-1} \mathbf{H}\right) \mathbf{P}\right]. \end{aligned} \tag{20}$$

A similar control scheme using gradient descent of $\mathcal{J}_{\mathbf{II}}$ can be obtained as

$$\dot{\mathbf{x}} = -k \nabla_{\mathbf{x}} \mathcal{J}_{\mathbf{II}}(\mathbf{x}, \mathcal{G}) = -k \frac{\partial}{\partial \mathbf{x}} \det(\mathbf{P}(\mathbf{x})) \tag{21}$$

5.1 Optimal Formations in $\mathbb{R}$

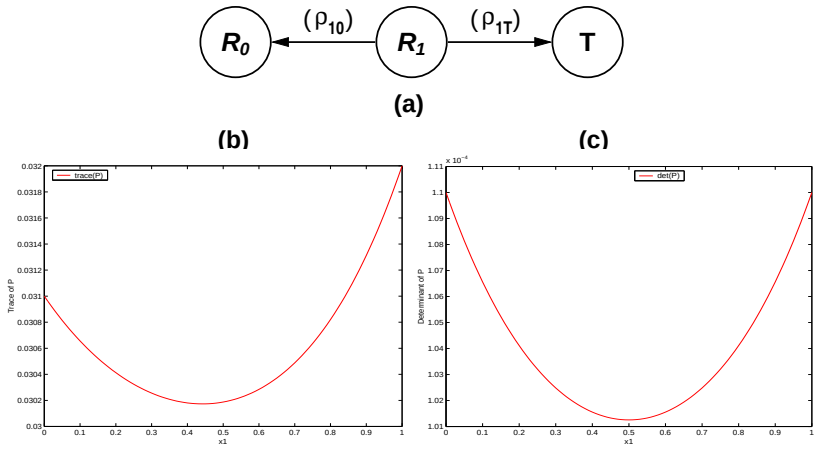

Fig. 6. (a) A candidate sensing graph for the single robot example in $\mathbb{R}$. (b) Uncertainty of position estimates of R_1 and the target, using $\mathcal{J}_{\mathbf{I}}$ =trace($\mathbf{P}(\mathbf{x})$) as the utility measure. (c) Uncertainty of position estimates of R_1 and the target, using $\mathcal{J}_{\mathbf{II}} = \det(\mathbf{P}(\mathbf{x}))$ as the utility measure.

As an example, we consider a single robot, R_1, and a target, T, in $\mathbb{R}$. Assume that the robot can measure the range between the origin R_0 at $x_0 = 0$ and itself, and the distance to the target at $x_T = 1$. The goal is to estimate the positions of the robot and target simultaneously while minimizing the overall estimation uncertainty. Figure 6 shows that the optimal position for R_1 to take the measurements is where the estimation uncertainty becomes minimal. And the point where the estimation uncertainty goes to minimum varies if a different utility measure for localization quality is used.

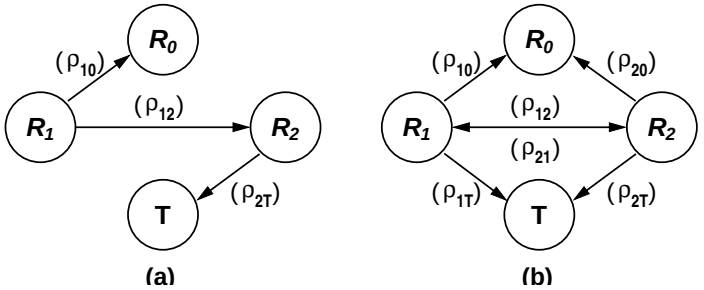

Fig. 7. (a) Sensing graph $\mathcal{G}_1$ for the two-robot formation. (b) Sensing graph $\mathcal{G}_2$ for the two-robot formation.

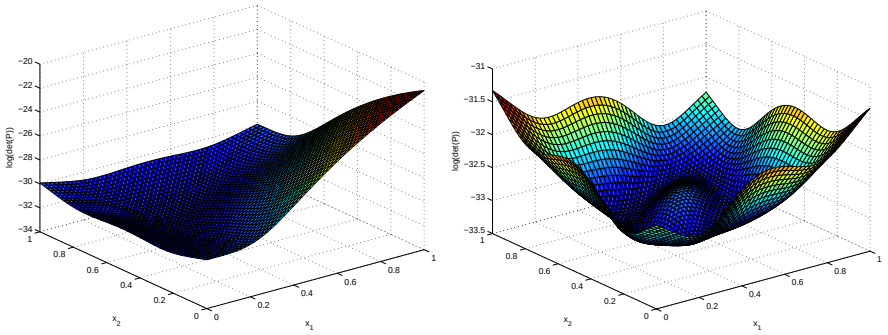

Fig. 8. (a) Uncertainty of position estimates under sensing graph $\mathcal{G}_1$. (b) Uncertainty of position estimates under sensing graph $\mathcal{G}_2$.

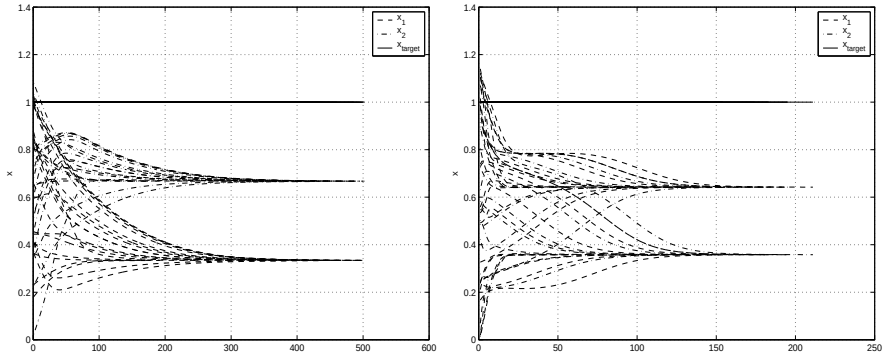

Fig. 9. (a) The trajectories of R_1 and R_2 in 1D space under sensing graph $\mathcal{G}_1$. (b) The trajectories of R_1 and R_2 in 1D space under sensing graph $\mathcal{G}_2$.

Another example of a two-robot formation in $\mathbb{R}$ is shown in Figure 7. In this example, a team of two robots, R_1 and R_2, are deployed to estimate the positions of themselves and a target at $x_T = 1$. Given two different sensing graphs as shown in Figure 7, the optimal shape of this two-robot formation

in $\mathbb{R}$ can be obtained analytically by solving for the minimum of the utility measure, $\mathcal{J}_{\mathbf{II}} = \det(\mathbf{P}(\mathbf{x}))$, which is represented by the surfaces in Figure 8. In Figure 9, we can see that using the gradient control as defined in Equation (21), robot R_1 and R_2 are distributed to the optimal positions where the minimum of the utility measure occurs in Figure 8.

5.2 Optimal Formations in $\mathbb{R}^2$

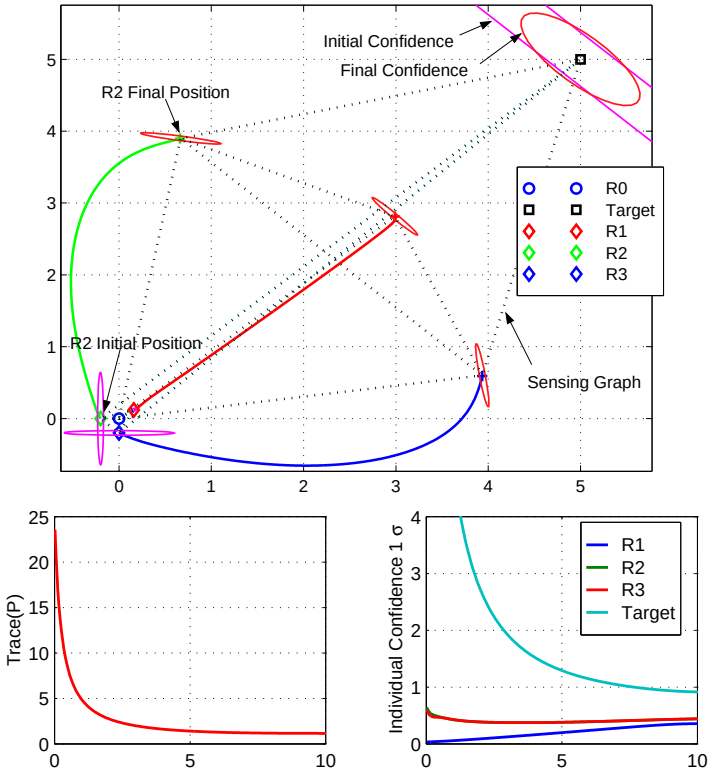

Fig. 10. Three mobile robots/sensors deploy to collectively localize themselves and a target of interest using a sensing graph containing the relative measurements $z = \{\phi_{10},\ \rho_{10},\ \rho_{12},\ \rho_{13},\ \rho_{20},\ \rho_{23},\ \rho_{2T},\ \rho_{30},\ \rho_{3T}\}$. Where ρ_{iT} denotes the relative range measurement between the i_{th} robot and the target.

As shown in Figure 10, three mobile robots, R_1, R_2, and R_3, are deployed to collaboratively localize themselves and a target of interest in the fixed beacon R_0's reference frame. A minimum number of relative measurements are used to achieve the localization. The initial compact formation of R_1, R_2 and R_3 close to R_0 yields poor target localization degrading overall localization

performance. The control scheme described by Equation (20) is applied to improve this situation. Each robot moves along a trajectory governed by the gradient of the trace of the error covariance matrix. The configuration of this mobile sensor network converges to an optimal formation, where the quality of overall team location estimation is maximized.

6 Discussion

There are many interesting challenges in networks of robots with sensors that go beyond the problems in sensor networks. Sensors generally have a limited range and field of view and their accuracy often varies with range. Depending on the information that needs to be acquired, robots/sensors can be positioned appropriately and even optimally. This paper presents a general framework and algorithms for controlling a network of robots to obtain relative position and orientation. While the main focus is on camera networks and problems in two dimensions, a similar approach can be used in three dimensions and for other sensors with different noise characteristics. With a suitable performance function, one can optimally configure robots to ensure every robot can localize itself relative to its neighbors and with respect to one or more targets.

There are many directions for future research. Throughout this paper, we assume that the sensing graph is invariant under robot motions. Though this is valid for some applications with particular kinds of sensors, it is generally not practical for sensors that are limited in terms of field of view and for robots with limited range of communication. For example, the effective range of the omni-directional cameras considered in Section 3 is less than 3 meters. Stereo cameras may have a larger range of sensing but they also have their limits. Occlusion due to obstacles may introduce changes in visibility and therefore changes in the network. Changes in the sensing graph in turn introduce discontinuities and make the control problem non-smooth.

Additionally, we have assumed that all robots can communicate with each other at all times. This may not be true, especially with small robots with low-power antennae. If multi-hop communication schemes are considered, robots may be able to talk to each other if they are all connected. Multi-hop introduces delays and noise that will adversely affect the control algorithm. Thus the choice of sensing graph will have to reflect the ease with which observations can be integrated and fused and the utility/cost associated with integrating a robot's measurements.

On a related note, the estimation and control algorithms discussed in this paper are centralized. We have considered the localization of all the robots and the target and cost functions that incorporate all the associated errors. Further, our centralized control scheme assumes complete state feedback and centralized decision making that can potentially lead to a global optimal solution for robots' states. However, before our proposed scheme can be scaled

to larger teams, we must consider how these algorithms can be distributed between robots so each robot can develop local estimates of state and independently make decisions on how to move to improve its estimates. The decentralized architecture for fusing sensory information and the coordinated control strategy for air-ground coordination proposed in [21] offer a starting point in this direction.

Finally, it is important to reiterate the lesson learned from the simple examples in Section 5. Even for the centralized minimization problem associate with two robot sensors operating on a line, there may be more than one local optimum. For multiple robots operating in two and three dimensions, schemes such as the one proposed in Equation (20) can only lead to local optima. There may be geometric singularities in configuration space associated with observation equations becoming functionally dependent. And as discussed above, it is necessary to change the sensing graph to avoid such configurations. Thus, this paper provides a starting point to a rich set of problems in cooperative control.

7 Acknowledgments

This work was in part supported by: DARPA MARS NBCH1020012, ARO MURI DAAD19-02-01-0383, and NSF CCR02-05336.

References

1. A. Das, J. Spletzer, , V. Kumar, and C. Taylor. Ad hoc networks for localization and control. In *Proceedings of the 41st IEEE Conference on Decision and Control, Las Vegas, NV*, 2002.
2. S.I. Roumeliotis and G. Bekey. Distributed multi-robot localization. In *IEEE Transactions on Robotics and Automations*, pages 781–795, 2002.
3. A. Howard, M. Matari, and C. Sukhatme. Team localization: a maximum likelihood approach. In *Technical Report IRIS-01-415, Institute for Robotics and Intelligent Systems Technical Report, University of Sourthern California*, 2002.
4. Ashley W. Stroupe, Martin C. Martin, and Tucker Balch. Distributed sensor fusion for object position estimation by multi-robot systems. In *Proceedings of the IEEE International Conference on Robotics and Automation*, pages 1092–1098, 2001.
5. J. Spletzer and C.J. Taylor. Dynamic sensor planning and control for optimally tracking targets. *International Journal of Robotics Research*, 22:7–20, 2003.
6. B. Grocholsky, A. Makarenko, T. Kaupp, and H.F. Durrant-Whyte. Scalable control of decentralised sensor platforms. In *Information Processing in Sensor Networks: 2nd Int Workshop, IPSN03*, pages 96–112, 2003.
7. G.A.S. Pereira, V. Kumar, and M.F.M. Campos. Decentralized algorithms for multi-robot manipulation via caging. *International Journal of Robotics Research*, 2004.

8. L.E. Navarro-Serment, J.M. Dolan, and P.K. Khosla. Optimal sensor placement for cooperative distributed vision. In *Proceedings of International Conference on Robotics and Automation, New Orleans, Louisiana*, 2004.
9. P. Ogren, E. Fiorelli, and N.E. Leonard. Cooperative control of mobile sensor networks: adaptive gradient climbing in a distributed environment. *To appear in IEEE Transactions on Automatic Control*, August 2004.
10. C. Belta and V. Kumar. Abstraction and control for groups of robots. *IEEE Transactions on Robotics and Automation*, 2004.
11. J. Desai, J. Ostrowski, and V. Kumar. Modeling and control of formations of nonholonomic mobile robots. *IEEE Transactions on Robotics and Automations*, 17(6):905–908, December 2001.
12. J. Spletzer, A.K. Das, R. Fierro, C.J. Taylor, V. Kumar, and J.P. Ostrowski. Cooperative localization and control for multi-robot manipulation. In *IEEE/RSJ International Conference on Intelligent Robots and Systems*, pages 631–636, 2001.
13. G.A.S. Pereira, A.K. Das, V. Kumar, and M.F.M. Campos. Decentralized motion planning for multiple robots subject to sensing and communication constraints. In *Proceedings of the Second Multi-Robot Systems Workshop, Washington, DC, USA*, pages 267–278, March 2003.
14. G.J. Pappas, P. Tabuada, and P. Lima. Feasible formations of multi-agent systems. In *Proceedings of the American Control Conference, Arlington, Virginia*, 2001.
15. G. Laman. On graphs and rigidity of plane skeletal structures. *Journal of Engineering Mathematics*, 4:331–340, October 1970.
16. B. Roth. Rigidity and flexible frameworks. *The American Mathematical Monthly*, 88:6–21, January 1982.
17. W. Whiteley and T. Tay. Generating isostatic frameworks. *Structural Topology*, 11:21–69, 1985.
18. T. Eren, D. Goldenberg, W. Whiteley, Y. Yang, A.S. Morse, B.D.O. Anderson, and P.N. Belhumeur. Rigidity and randomness in network localization. In *Proceedings of the IEEE INFOCOM Conference, Hong Kong*, 2004.
19. R. Olfati-Saber and R.M. Murray. Graph rigidity and distributed formation stabilization of multi-vehicle systems. In *Proceedings of the IEEE Conference on Decision and Control*, 2002.
20. F. Zhang, B. Grocholsky, and V. Kumar. Formations for localization of robot networks. In *Proceedings of International Conference on Robotics and Automation, New Orleans, Louisiana*, 2004.
21. B. Grocholsky, S. Bayraktar, V. Kumar, C.J. Taylor, and G. Pappas. Synergies in feature localization by air-ground robot teams. In *Proceedings of the 9th International Symposium on Experimental Robotics, Singapore*, June 2004.